Accepted Manuscript

Scutellarin derivatives as apoptosis inducers: Design, synthesis and biological evaluation

Tong Han, Jia Li, Jingjing Xue, He Li, Fanxing Xu, Keguang Cheng, Dahong Li, Zhanlin Li, Ming Gao, Huiming Hua

PII: S0223-5234(17)30177-0

DOI: 10.1016/j.ejmech.2017.03.020

Reference: EJMECH 9280

To appear in: *European Journal of Medicinal Chemistry*

Received Date: 16 January 2017

Revised Date: 10 March 2017

Accepted Date: 11 March 2017

Please cite this article as: T. Han, J. Li, J. Xue, H. Li, F. Xu, K. Cheng, D. Li, Z. Li, M. Gao, H. Hua, Scutellarin derivatives as apoptosis inducers: Design, synthesis and biological evaluation, *European Journal of Medicinal Chemistry* (2017), doi: 10.1016/j.ejmech.2017.03.020.

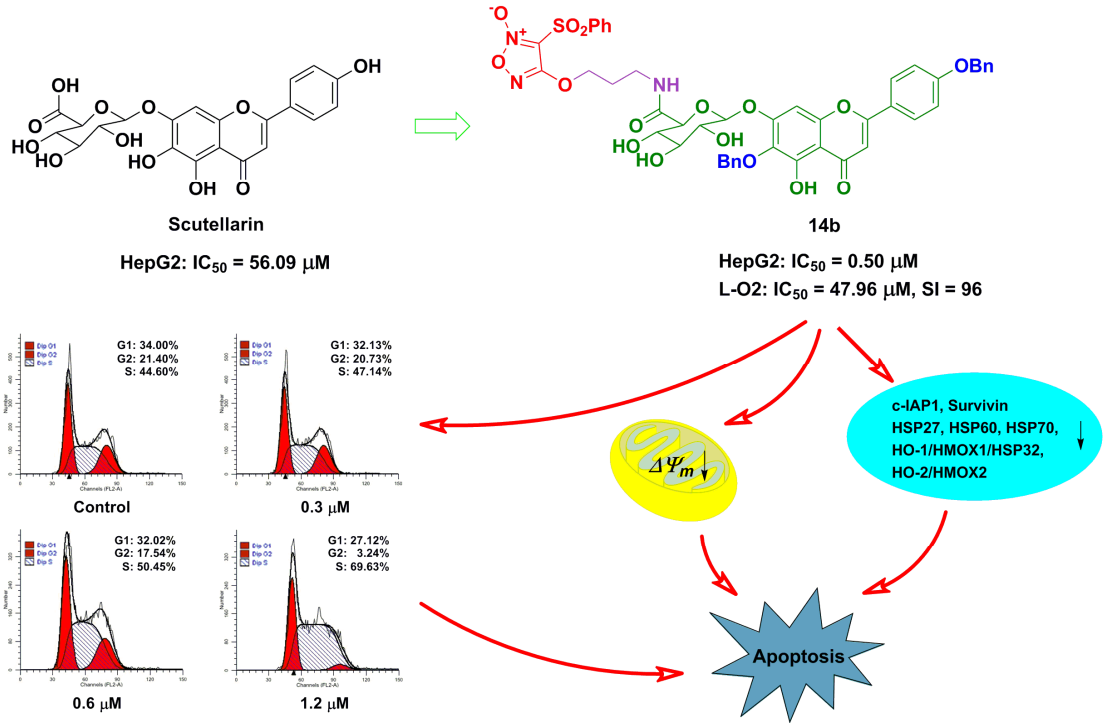

Scutellarin derivatives as apoptosis inducers: design, synthesis and biological evaluation

Tong Han[a], Jia Li[a], Jingjing Xue[a], He Li[a], Fanxing Xu[b,*], Keguang Cheng[c], Dahong Li[a,*], Zhanlin Li[a], Ming Gao[d] and Huiming Hua[a,*]

[a] *Key Laboratory of Structure-Based Drug Design & Discovery, Ministry of Education, and School of Traditional Chinese Materia Medica, Shenyang Pharmaceutical University, 103 Wenhua Road, Shenyang 110016, China*

[b] *Wuya College of Innovation, Shenyang Pharmaceutical University, 103 Wenhua Road, Shenyang 110016, China*

[c] *State Key Laboratory for the Chemistry and Molecular Engineering of Medicinal Resources, and School of Chemistry and Pharmacy, Guangxi Normal University, 15 Yucai Road, Guilin 541004, China*

[d] *School of Pharmaceutical Sciences, Mukogawa Women's University, 11-68 Koshien, Nishinomiya 663-8179, Japan*

[*] Corresponding authors. Tel.: +86-24-23986465; Fax: +86-24-23986465.

E-mail address: huimhua@163.com (H. Hua); lidahong0203@163.com (D. Li); fanxing0011@163.com (F. Xu).

Abstract:

To explore novel antitumor agents with high efficiency and low toxicity, a series of NO-donating scutellarin derivatives (**14**–**17**) were synthesized and the antiproliferative activities against MCF-7, HCT-116, PC-3 and HepG2 cancer cell lines were assessed. Among them, compound **14b** was the strongest with IC_{50} values of 2.96 μM, 7.25 μM, 0.09 μM and 0.50 μM, respectively, and displayed low toxicity against normal human liver L-O2 cells with an IC_{50} of 47.96 μM, showing good selectivity between normal and malignant liver cells. Moreover, NO releasing ability of the derivatives has been studied. Mechanism studies of the most promising compounds **14b** and **15a** were carried out. The results indicated that **14b** and could induce apoptosis, cell cycle arrest at the S phase and led to mitochondrial dysfunction in the HepG2 and PC-3 cell lines, respectively. Furthermore, Human Apoptosis Protein Array kit assay demonstrated that **14b** could induce apoptosis through down-regulating the levels of procaspase-3 and inhibiting the expression of survivin, c-IAP1, HSP27, HSP60, HSP70, HO-1/HMOX1/HSP32 and HO-2/HMOX2 in HepG2 cell line. These results guaranteed compound **14b** to be a drug candidate against liver cancer for further investigation.

***Key words*:** scutellarin, antiproliferative activity, selectivity, NO, apoptosis.

1. Introduction

Natural products have been the major sources of chemical diversity for lead compounds, inspiring for the research and development of new drugs [1,2]. According to the statistics, there are nearly 51% of currently marketed drugs owing their origins to natural compounds [3]. Flavonoids, as a large class of natural products, are widely distributed in the plant kingdom as secondary metabolites [4]. They show various biological activities, especially for the treatment of cancer [5], cardiovascular diseases [6] and neurodegenerative disorders [7]. Moreover, flavonoids are considered to exhibit positive impact on human health without significant side effects, since they are also existed in fruits and vegetables which we consume inadvertently in our daily diet [8,9].

Scutellarin, an extract from traditional Chinese herb *Erigeron breviscapus* (*vant.*) Hand-Mazz, is the main effective flavonoid component of breviscapine [10]. It has been widely reported for the treatment of cardiovascular diseases, such as hypertension [11], myocardial fibrosis [12,13] and cardiomyocyte ischemia/reperfusion injury [14,15]. Recently, scutellarin was found to show anticancer activity [16,17], which could suppress proliferation, migration and invasion of human hepatocellular carcinoma cells *via* inhibiting the STAT3/Girdin/Akt activity [18,19]. There were also accumulating evidences suggesting that scutellarin could significantly inhibit the growth, adhesion and migration of human tongue squamous carcinoma cells by reducing the expression of MMP-2, MMP-9 and integrin $\alpha_v\beta_6$ [20,21,22]. All these results demonstrated that scutellarin possessed potent antitumor activities with great therapeutic potentials. However, some perceived disadvantages of scutellarin limited its further application, mainly including low stability and poor oral bioavailability [23]. In order to overcome these disadvantages, methyl and benzyl as protective groups were introduced to 6-OH and 4′-OH in order to avoid oxidation, and the antitumor activities of the modified derivatives could also be further improved since methyl and benzyl groups were benefit to the antitumor activity of flavonoid derivatives according to the literatures [24,25].

Nitric oxide (NO) is a low molecular weight signaling molecule and plays pivotal roles in

diverse physiological and pathophysiological processes [26]. Over the past decade, NO has aroused great interest as a potential antitumor agent [27]. The molecular mechanisms involved in NO-mediated cell death are multiple. In general, high concentration of NO can induce apoptosis, inhibit metastasis of tumor cells, and sensitize tumor cells to chemotherapy, radiation and immunotherapy [28,29]. Some kinds of NO donors can produce high levels of NO with a wide range of half-lives *in vitro* and *in vivo*, and have been widely used in drug research, especially the types of furoxan and nitrate [29-31]. Furoxans are an important class of thermodynamically stable NO donors. A variety of active compounds or natural products including bifendate, coumarin and oleanolic acid have been hybrided with furoxan (Figure 1) and displayed potent antitumor activities [32-34]. Another kind of important NO donors with a long history, nitrates, can also exert great influence in the treatment of tumor, such as some oleanolic acid derivatives (Figure 1) [35]. Hence, design and synthesis of NO-releasing based hybrids is an effective and promising strategy for cancer treatment [36]. As an important class of natural products with a variety of biological activities, flavonoids are attractive to many researchers. Some NO-donating derivatives of flavonoids were reported as well, for instance, the nitrate derivatives of apigenin, chrysin and luteolin were found to prevent the development of diabetic complications [37,38]. However, there were only a few reports concerning the antitumor activity of NO-donating flavoid derivatives [39].

On the basis of these reasons, we synthesized 12 new scutellarin derivatives **14**–**17** with furoxan or nitrate moiety through different linkers and evaluated their antiproliferative activities by MTT assay against human tumor MCF-7, HCT-116, PC-3, HepG2 cells and normal liver L-O2 cells. Furthermore, the NO-releasing ability and the mechanisms concerning cell cycle progression, induction of apoptosis and effects on apoptosis-related proteins by representative derivatives were investigated.

2. Results and discussion

2.1. Chemistry

The synthetic routine of target compounds is illustrated in Scheme 1. **5** was synthesized in a

three-step sequence according to the literature [40], and then converted to various monophenylsulfonylfuroxans (**6a–d**) by treatment with corresponding amino-substituted alcohol (ethanolamine, 3-aminopropanol, 1-aminopropan-2-ol and *N*-(2-hydroxyethyl)piperazine) (Scheme 1). 2-Bromoethanol and 3-bromo-1-propanol were treated with HNO_3 and H_2SO_4 in CH_2Cl_2 to give its mononitrates **9a** and **9b** (Scheme 2).

Scutellarin was used as the raw material, and compound **10** and **11** were prepared by reacted with benzyl bromide and methyl iodide. Then they were hydrolyzed by KOH to generate the intermediates **12** and **13**. Finally, the furoxan (**6a**–**d**) and nitrate (**9a** and **9b**) intermediates were treated with the derivatives (**12** and **13**) of scutellarin to give the target compounds **14a**–**d**, **15a**–**d**, **16a**, **16b**, **17a** and **17b** (Scheme 3). The structures of all the derivatives were confirmed by ^{1}H NMR, ^{13}C NMR and high resolution mass spectrum (HR-MS).

2.2. Biological evaluation

2.2.1 Antiproliferative activity

Twelve new scutellarin/furoxan or nitrate hybrids (**14a**–**d**, **15a**–**d**, **16a**, **16b**, **17a** and **17b**) were evaluated for their inhibitory effects against four different human cancer cell lines (human breast carcinoma cell line MCF-7, human colorectal carcinoma cell line HCT-116, human prostatic cancer cell line PC-3 and human liver carcinoma cell line HepG2), in comparison with the reference 5-FU. Meanwhile, the activities against the human normal hepatic cell line (L-O2) were also evaluated since a potential anticancer drug candidate would be better to show selective cytotoxicity between malignant and normal cells.

As shown in Table 1, most target compounds displayed more potent inhibitory activities than scutellarin, and some of them showed superior cytotoxic activities to 5-FU. The furoxan hybrids **14a**–**d** and **15a**–**d** showed significant antiproliferative activities against four cancer cell lines with IC_{50} values ranging from 0.09 μM to 39.97 μM, especially against PC-3 (IC_{50} 0.09 μM–3.65 μM) , HCT-116 (IC_{50} 1.27 μM–13.58 μM) and HepG2 (IC_{50} 0.50 μM–12.92 μM) cells. Compounds

14a–d with benzyl groups at the 6- and 4′-hydroxyl of scutellarin displayed more potential activities against MCF-7, PC-3 and HepG2 cells than corresponding ones with methyl groups. The results were in accord with previous literatures that bulky benzyl group was preferred for antiproliferative activity [24,25]. Interestingly, the antiproliferative activities showed almost no differences among compounds **14a**, **14b**, **14c** and **14d** (**15a**, **15b**, **15c** and **15d**) against most cancer cell lines when the linkers were changed. Notably, compound **14b** displayed the most potent antiproliferative activity among compounds **14a–d**, with IC_{50} values of 0.09 μM–7.25 μM, especially against PC-3 (IC_{50} 0.09 μM) and HepG2 cells (IC_{50} 0.50 μM). Compounds **15a–d** showed comparable antitumor potency to 5-FU against HCT-116 cell line and more potent activities against PC-3 and HepG2 cell lines. On the other hand, nitrate hybrids **16a**, **16b**, **17a** and **17b** exhibited no significant activity against any of the selected cancer cell lines, except for compound **16b** showing moderate inhibitory activity against HCT-116 cells with IC_{50} of 17.40 μM.

In addition, to investigate whether the hybrids exhibited selective antiproliferative activities between normal and malignant liver cells, **14a–d** and **15a–d** were screened against human normal liver L-O2 cells with scutellarin as control. The results were listed in Table 1. All the tested compounds showed low antiproliferative activities against L-O2 cells with IC_{50} values from 19.31 μM to 47.96 μM. In particular, compound **14b** displayed 96-fold less antiproliferative activity against nontumor L-O2 cells than HepG2 tumor cells.

2.2.2. NO-releasing ability in vitro

The levels of NO released by the target compounds were tested by Griess assay [41]. As shown in Table 2, generally, the series of furoxan-based NO donor hybrids (**14a–d** and **15a–d**) displayed more potent NO-releasing ability than the series bearing nitrate moiety (**16a**, **16b**, **17a** and **17b**). This indicated that the antiproliferative activities would be partly attributed to the NO releasing ability. Meanwhile, the derivatives **15a–d** with 6- and 4'-hydroxyl substitutions of methyl groups were found to release more NO than **14a–d** with benzyl groups. These results

suggested that the benzyl groups might hinder the metabolism of furoxans. Compound **14b** which showed the strongest growth inhibitory activity also produced a sustained release of more than 20 μM/L of NO at the time point of 3 h. The maximum amount of NO was produced by compound **15a** with above 59 μM/L at the time point of 3 h. In addition, we determined the intracellular NO levels produced by compounds**14a**–**d** and **15a**–**d** in HepG2 and L-O2 cells. As shown in Figure 2, all the derivatives released more than 26.3 μM/L of NO at the time point of 1 h in HepG2 cell, and less than 15.46 μM/L of NO in L-O2 cells. These results indicated that relatively high levels of NO produced by the scutellarin derivatives were benifit to their strong antiproliferative activities. In order to investigate the mechanism of action, the functions of compound **14b** in HepG2 cells and **15a** in PC-3 cells were chosen for further study.

2.2.3. Cell cycle analysis

The effects on the cell cycle distribution in HepG2 and PC-3 cells were first evaluated. HepG2 and PC-3 cells were treated with compound **14b** (0, 0.3, 0.6 and 1.2 μM) and compound **15a** (0, 0.16, 0.31 and 1.25 μM) for 72 h, respectively, then stained with propidium iodide (PI) and analyzed by flow cytometry. Non-treated cells were used as control. As shown in Figure 3, cells in the S phase increased from 44.60% in control group to 47.14%, 50.45% and 69.63% in a concentration-dependent manner in HepG2 cell lines. These results revealed that compound **14b** caused S phase arrest in a concentration-dependent manner. At the same time, the similar results were observed by compound **15a** in PC-3 cell line that the cell cycle was significantly arrested in the S phase.

2.2.4. The morphological analysis by Hoechst 33258 staining

The changes of morphological features, such as cell shrinkage, chromatin condensation, nuclear membrane blebbing are the characteristics of apoptotic cells [42]. Hoechst 33258, which stains the cell nuclei and emits fluorescence allowing the visualization of nuclear morphological

changes, is a membrane permeable dye. Hence, we used fluorescence microscopy to observe the morphology of HepG2 and PC-3 cells stained with Hoechst, after treatment with different concentrations (same as the cell cycle test) of compounds **14b** and **15a**, respectively, for 48 h.

The morphological analysis, depicted in Figure 4, showed that control cells were uniformly stained with Hoechst 33258 and presented round homogeneous nuclei, without morphological changes. HepG2 cells were exposed to 0.3 μM and 0.6 μM of compound **14b** for 48 h, which presented remarkable morphological changes, such as cell shrinkage, chromatin condensation and evident reduction in the number of adherent cells. The rupture of cell membrane and the nuclear fragmentation were evident after the treatment of HepG2 cells with 1.2 μM of compound **14b**. These typical apoptotic morphology changes were also observed in different concentrations of **15a** treated PC-3 cells. These results strongly supported the pro-apoptotic effects of compounds **14b** and **15a**.

2.2.5. Cell apoptosis assay

Since high levels of NO induce cellular apoptosis [43], the cellular apoptosis ability of **14b** and **15a** were tested. The cells were treated with different concentrations (same as the cell cycle test) of compounds **14b** or **15a** for 72 h. Then, the cells were harvested and stained with 7-aminoactinomycin D (7-AAD) and annexin-V, and the percentages of apoptotic cells were determined by flow cytometry analysis. As shown in Figure 5 (A, B), the treatment of HepG2 cells with compound **14b** at concentrations of 0.3, 0.6 and 1.2 μM for 72 h resulted in cell apoptosis at the ratios of 16.54%, 33.1% and 52.62%, respectively, as compared with 8.05% in the control group. And the treatment of PC-3 cells with 1.25 μM of compound **15a** decreased the percentage of live cells from 88.74% to 36.34% and increased the apoptotic cells from 8.83% to 58.45% (14.91% of earlier apoptotic cells and 43.54% of late apoptotic cells). These results showed that compounds **14b** and **15a** caused a marked increase of the cellular apoptosis in a concentration-dependent manner in HepG2 and PC-3 cells, respectively.

Morover, the effects of apoptosis in normal human liver cells L-O2 induced by **14b** or **15a**

were also tested. As shown in Figure 5 (C), when L-O2 cells were treated with compounds **14b** and **15a** at the concentrations of 1.2 μM and 1.25 μM, respectively, almost no cellular apoptosis was observed. However, at the same concentrations, they can induce apoptosis obviously in HepG2 and PC-3 cells. These data comfirmed the good selectivity of compounds **14b** and **15a** between normal and malignant liver cells.

2.2.6. Mitochondria membrane potential ($\Delta\psi_m$)

Mitochondria play a crucial role in the induction and control of apoptosis, which results in a variety of key events, including the loss of mitochondrial membrane potential ($\Delta\psi_m$) and release of pro-apoptotic factors such as cytochrome c and other apoptosis-inducing factors [44]. NO is also known to induce apoptosis by activating the intrinsic mitochondrion-mediated pathways [45]. We therefore studied the effects on mitochondrial membrane potential of target compounds **14b** and **15a** in HepG2 and PC-3 cell lines, respectively. The cells were treated with different concentrations (same as the cell cycle test) of **14b** and **15a** for 48 h, respectively, and the changes of mitochondrial membrane potential ($\Delta\psi_m$) were monitored by flow cytometry using the dye 5,5′,6,6′-tetrachloro-1,1′,3,3′-tetraethylbenzimidazol-caebocyanine (JC-1). As shown in Figure 6 in HepG2 and PC-3 cells, compounds **14b** and **15a** induced a concentration-dependent increase in the proportion of cells with depolarized mitochondria. This illustrated that the induction of apoptosis by hybrids **14b** and **15a** was associated with the mitochondrial (intrinsic) pathways.

2.2.7. Quantitation of cellular proteins involved in apoptosis

Apoptosis is an essential physiological cell death process in development, homeostasis, and immune defense of multicellular animals [46]. To better understand the mechanism of scutellarin derivatives, we performed a protein array assay using the Human Apoptosis Protein Array kit. Compound **14b** was chosen for this study in HepG2 cells. The visible changes of some apoptotic proteins were observed (Figure 7) and the whole experimental results were presented in the

supporting materials (Figure S1)。

Caspases are key factors in apoptotic cell death. Caspase-3 in particular, can be activated by the proteolytic processing of procaspase-3 in response to exogenous apoptosis inducers [47]. The inhibitors of apoptosis proteins (IAP), a family of anti-apoptotic regulators, express at high levels and prevent caspase-mediated apoptosis in cancer cells. The human IAP family contains eight proteins: c-IAP1, c-IAP2, NAIP, survivin, XIAP, bruce, ILP-2 and livin [48,49]. As shown in Figure 7, the results indicated that caspase-3 was activated because of decreased expression of procaspase-3 after the treatment of **14b** for 24 h. Moreover, in comparison with the control cells, **14b** induced a significant reduction in the levels of survivin and c-IAP1.

Heat shock proteins (HSPs), especially Hsp 27, Hsp 60, Hsp 70 and Hsp 90, are not only involved in normal physiology but also in cancer [50-52]. They can inhibit the activity of caspases directly or indirectly, thereby blocking the intrinsic and extrinsic apoptotic pathways through interaction with key apoptotic proteins [53,54]. Heme oxygenase (HO) is a cytoprotective enzyme that can be overexpressed in cancer cells and promotes proliferation and survival. Two isoenzymes of HO, the inducible form HO-1 and the constitutive form HO-2, have been well characterized [55-57]. The effects of compound **14b** on the constitutive levels of HSPs and HO in HepG2 cells are shown in Figure 7. Exposure of HepG2 cells to compound **14b** caused a dramatic decrease in the levels of Hsp27, Hsp 60, Hsp 70, HO-1 and HO-2, as compared with control. These observations suggested that compound **14b** might induce HepG2 cells apoptosis through caspase cascade and inhibit the expression of anti-apoptotic proteins.

3. Conclusion

In summary, a series of hybrids of scutellarin and NO donors (furoxans or nitrate) (**14a**–**d**, **15a**–**d**, **16a**,**b** and **17a**,**b**) were synthesized and evaluated. Most of them showed strong antiproliferative activities against four cancer cell lines (MCF-7, HCT-116, PC-3 and HepG2) and weak cytotoxic activities against human normal liver cell line L-O2. Particularly, for compound **14b**, exhibited the best selectivity with the selective index of 96. In addition, **14b** showed

sustained NO releasing ability in the Griess assay and compound **15a** produced the greatest amount of NO of above 59 μM/L by the time point of 3 h. Hence, compounds **14b** and **15a** were chosen for further investigation in order to reveal the cellular mechanisms in different cell lines. The apoptosis-inducing activity of representative compounds **14b** in HepG2 cells and **15a** in PC-3 cells were tested. The results demonstrated that hybrids **14b** and **15a** showed similar effects which could induce cell apoptosis and arrest cell cycle at the S stage. Human Apoptosis Protein Array kit was further applied to disclose the effects of apoptosis-related proteins by compound **14b** in HepG-2 cells. The results suggested that compound **14b** induced HepG-2 cells apoptosis through down-regulation of the level of pro-caspase-3 and inhibited the expression of anti-apoptotic proteins (c-IAP1, survivin, HSP27, HSP60, HSP70, HO/HMOX1/HSP32 and HO-2/HMOX2). Consequently, the rational design of scutellarin derivatives containing NO-donating moiety offered a good strategy for the discovery of antitumor agents with high efficiency and low toxicity.

4. Experimental

4.1. Chemistry

Melting points (mp) were determined on an X-4 melting point apparatus and uncorrected. ^{1}H NMR and ^{13}C NMR spectra were measured on Bruker ARX-300, AV400 MHz or ARX-600 spectrometers with tetramethylsilane (TMS) as the internal standard. Chemical shifts were reported in δ (ppm). Mass spectra (MS) were determined on Finnigan MAT/USA spectrometer (LC-MS). High-resolution mass spectra were obtained on Bruker microOTOF-Q in the ESI mode (HR-ESI-MS). Scutellarin was purchased from Jiangsu Zelang Bio-pharm. Pty. Ltd. China, with the purity over 95%. The other reagents were obtained from commercial suppliers and used without purification. TLC analysis was carried out on silica gel plates GF254 (Qindao Haiyang Chemical, China). Column chromatography was performed on silica gel (200–300 mesh). Compounds **6a**–**d**, **9a**,**b** and intermediates **10**–**13** were prepared as described previously [37], and

their chemical characterizations were shown in the Supplementary materials.

*4.1.1. General procedure for the synthesis of compounds **14a-d** and **15a-d***

A mixture of **12** or **13** (0.5 mmol) and HOBt (0.6 mmol) in anhydrous DMF (5 mL) was stirred at room temperature for 0.5 h. After the addition of 4-(2-aminoethoxy)-3-(phenylsulfonyl)-1,2,5-oxadiazole-2-oxide (**6a**), 4-(3-aminopropoxy)-3-(phenylsulfonyl)-1,2,5-oxadiazole-2-oxide (**6b**), 4-((1-aminopropan-2-yl)oxy)-3-(phenylsulfonyl)-1,2,5-oxadiazole-2-oxide (**6c**) or 3-(phenylsulfonyl)-4-(2-(piperazin-1-yl)ethoxy)-1,2,5-oxadiazole-2-oxide (**6d**) (0.75 mmol) and EDCI (0.75 mmol) to the solution, the mixture was further stirred at room temperature for 3 h. Then, the mixture was poured into 20 mL of H_2O, and extracted with EtOAc (3 × 20 mL). The organic layer was combined, washed with brine, dried over anhydrous Na_2SO_4, and concentrated in vacuo. The crude product was purified on silica gel column chromatography eluting with dichloromethane/methanol system.

*4.1.1.1. 4-(2-(-6-((6-(Benzyloxy)-2-(4-(benzyloxy)phenyl)-5-hydroxy-4-oxo-4H-chromen-7-yl)oxy)-3,4,5-trihydroxytetrahydro-2H-pyran-2-carboxamido)ethoxy)-3-(phenylsulfonyl)-1,2,5-oxadiazole-2-oxide (**14a**).*

Yellow power, 241 mg; yield: 53.1%, mp: 179–181 ^{o}C; MS(ESI) *m/z*: 910.2 $[M + H]^+$, 932.2 $[M + Na]^+$; HRMS (ESI) *m/z* calcd for $C_{45}H_{39}N_3NaO_{16}S$ $[M + Na]^+$ 932.1943, found 932.1943; ^{1}H NMR (DMSO-d_6, 400 MHz) δ (ppm): 12.95 (s, 1H, 5-OH), 8.23 (t, 1H, *J* = 5.6 Hz, -NH-), 8.02 (d, 2H, *J* = 8.9 Hz, H-2′,6′), 7.95 (d, 2H, *J* = 7.4 Hz, Ar-H), 7.75 (t, 1H, Ar-H), 7.65 (d, 2H, *J* = 7.4 Hz, Ar-H), 7.56 (d, 2H, *J* = 6.6 Hz, Ar-H), 7.47 (d, 2H, *J* = 7.4 Hz, Ar-H), 7.43–7.31 (m, 6H, Ar-H), 7.17 (d, 2H, *J* = 8.9 Hz, H-3′,5′), 7.12 (s, 1H, H-8), 6.95 (s, 1H, H-3), 5.65 (brs, 1H, H-1″), 5.37–5.31 (m, 3H, sugar hydroxyl), 5.21 (s, 2H, -CH_2-), 5.09 (d, 1H, *J* = 10.9 Hz, -CH_2-), 4.98 (d, 1H, *J* = 10.9 Hz, -CH_2-), 4.43 (t, 2H, -CH_2-), 4.06 (d, 1H, *J* = 9.7 Hz, H-5″), 3.62–3.52 (m, 3H, H-2″, 3″, 4″), 3.44 (t, 2H, -CH_2-). ^{13}C NMR (DMSO-d_6, 100 MHz) δ (ppm): 182.79, 169.19, 164.28, 161.94, 159.18, 156.75, 153.30, 152.72, 138.05, 137.35, 136.91, 136.36, 131.82, 130.76,

130.42, 130.35, 130.35, 129.21, 128.97, 128.97, 128.87, 128.87, 128.57, 128.57, 128.51, 128.51, 128.30, 128.30, 123.37, 115.79, 115.79, 111.06, 111.06, 106.39, 103.87, 100.21, 94.51, 76.64, 76.27, 74.66, 73.36, 71.70, 70.03, 69.93, 67.87.

*4.1.1.2. 4-(3-(6-((6-(Benzyloxy)-2-(4-(benzyloxy)phenyl)-5-hydroxy-4-oxo-4H-chromen-7-yl)oxy)-3,4,5-trihydroxytetrahydro-2H-pyran-2-carboxamido)propoxy)-3-(phenylsulfonyl)-1,2,5-oxadiazole-2-oxide (**14b**).*

Yellow power, 210 mg; yield: 45.5%, mp: 127–129 ^{o}C; MS(ESI) *m/z*: 924.2 $[M + H]^+$, 946.2 $[M + Na]^+$; HRMS (ESI) *m/z* calcd for $C_{46}H_{42}N_3O_{16}S$ $[M + H]^+$ 946.2100, found 946.2089; ^{1}H NMR (DMSO-d_6, 400 MHz) δ (ppm): 12.97 (s, 1H, 5-OH), 8.19 (t, 1H, *J* = 5.7 Hz, -NH-), 8.05 (d, 2H, *J* = 8.9 Hz, H-2′,6′), 7.98 (d, 2H, *J* = 7.4 Hz, Ar-H), 7.81 (t, 1H, Ar-H), 7.69 (d, 2H, *J* = 7.9 Hz, Ar-H), 7.56 (d, 2H, *J* = 6.8 Hz, Ar-H), 7.47 (d, 2H, *J* = 6.8 Hz, Ar-H), 7.40–7.35 (m, 6H, Ar-H), 7.18 (d, 2H, *J* = 8.9 Hz, H-3′,5′), 7.07 (s, 1H, H-8), 6.95 (s, 1H, H-3), 5.64 (brs, 1H, H-1″), 5.44–5.27 (m, 3H, sugar hydroxyl), 5.21 (s, 2H, -CH_2-), 5.08 (d, 1H, *J* = 10.8 Hz, -CH_2-), 4.96 (d, 1H, *J* = 10.8 Hz, -CH_2-), 4.34 (t, 2H, -CH_2-), 3.96 (d, 1H, *J* = 9.6 Hz, H-5″), 3.53–3.45 (m, 3H, H-2″,3″,4″), 3.24 (t, 2H, -CH_2-), 1.90 (m, 2H, -CH_2-). ^{13}C NMR (DMSO-d_6, 100 MHz) δ (ppm): 182.82, 168.55, 164.27, 162.00, 159.21, 156.73, 153.28, 152.72, 138.02, 137.55, 136.90, 136.53, 132.06, 131.80, 130.45, 130.45, 129.12, 128.96, 128.96, 128.87, 128.87, 128.80, 128.57, 128.57, 128.50, 128.50, 128.29, 128.29, 123.35 , 115.80, 115.80, 110.85, 110.85, 106.39, 103.86, 100.39, 94.54, 76.81, 76.52, 74.64, 73.41, 71.40, 70.04, 69.42, 67,86, 52.47.

*4.1.1.3. 4-((1-(6-((6-(Benzyloxy)-2-(4-(benzyloxy)phenyl)-5-hydroxy-4-oxo-4H-chromen-7-yl)oxy)-3,4,5-trihydroxytetrahydro-2H-pyran-2-carboxamido)propan-2-yl)oxy)-3-(phenylsulfonyl)-1,2,5-oxadiazole-2-oxide (**14c**).*

Yellow power, 306 mg; yield: 66.3%, mp: 135–137 ^{o}C; MS(ESI) *m/z*: 924.1 $[M + H]^+$, 946.2 $[M + Na]^+$; HRMS (ESI) *m/z* calcd for $C_{46}H_{41}N_3NaO_{16}S$ $[M + Na]^+$ 946.2100, found 946.2097; ^{1}H NMR (DMSO-d_6, 400 MHz) δ (ppm): 12.96 (s, 1H, 5-OH), 8.23 (t, 1H, -NH-), 8.05 (d, 2H, *J* = 8.9 Hz, H-2′,6′), 7.97 (d, 2H, *J* = 7.3 Hz, Ar-H), 7.77 (t, 1H, Ar-H), 7.68 (d, 2H, *J* = 7.4 Hz, Ar-H),

7.57 (d, 2H, *J* = 7.0Hz, Ar-H), 7.48 (brs, 2H, Ar-H), 7.43–7.33 (m, 6H, Ar-H), 7.18 (d, 2H, *J* = 8.9 Hz, H-3′,5′), 7.06 (s, 1H, H-8), 6.94 (s, 1H, H-3), 5.65 (d, 1H, *J* = 5.2 Hz, H-1″), 5.42–5.27 (m, 3H, sugar hydroxyl), 5.21 (s, 2H, -CH_2-), 4.96 (dd, 2H, *J* = 10.6 Hz, -CH_2-), 4.23 (m, 1H, -CH-), 4.03 (d, 1H, *J* = 9.0 Hz, H-5″), 3.61–3.50 (m, 3H, H-2″,3″,4″), 3.43 (d, 2H, -CH_2-), 1.27 (t, 2H, -CH_3). ^{13}C NMR (DMSO-d_6, 100 MHz) δ (ppm): 182.82, 168.92, 164.28, 161.96, 158.66, 156.73, 153.29, 152.70, 138.04, 137.40, 136.90, 136.37, 131.85, 131.81, 130.44, 130.44, 129.06, 128.97, 128.97, 128.88, 128.88, 128.83, 128.57, 128.57, 128.51, 128.51, 128.30, 128.30, 123.33, 115.79, 115.79, 111.14, 111.14, 106.40, 103.87, 100.33, 94.72, 76.83, 76.27, 74.66, 73.46, 73.37, 71.57, 71.35, 70.03, 17.27.

*4.1.1.4. 4-(2-(4-(6-((6-(Benzyloxy)-2-(4-(benzyloxy)phenyl)-5-hydroxy-4-oxo-4H-chromen-7-yl)oxy)-3,4,5-trihydroxytetrahydro-2H-pyran-2-carboyl)piperazin-1-yl)ethoxy)-3-(phenylsulfonyl)-1,2,5-oxadiazole-2-oxide (**14d**).*

Yellow power, 150 mg; yield: 51.1%, mp: 123–125 ^{o}C; MS(ESI) *m/z*: 979.1 $[M + H]^+$, 1001.1 $[M + Na]^+$; HRMS (ESI) *m/z* calcd for $C_{49}H_{46}N_4NaO_{16}S$ $[M + Na]^+$ 1001.2522, found 1001.2512; ^{1}H NMR (DMSO-d_6, 400 MHz) δ (ppm): 12.92 (s, 1H, 5-OH), 8.02 (d, 2H, *J* = 8.9 Hz, H-2′,6′), 7.94 (d, 2H, *J* = 7.3 Hz, Ar-H), 7.82 (t, 1H, Ar-H), 7.68 (d, 2H, *J* = 7.9 Hz, Ar-H), 7.54 (d, 2H, *J* = 7.1 Hz, Ar-H), 7.45 (d, 2H, *J* = 7.1 Hz, Ar-H), 7.39–7.34 (m, 6H, Ar-H), 7.21 (s, 1H, H-8), 7.17 (d, 2H, *J* = 8.9 Hz, H-3′,5′), 6.93 (s, 1H, H-3), 5.67 (brs, 1H, H-1″), 5.53 (d, 1H, sugar hydroxyl), 5.28 (brs, 1H, sugar hydroxyl), 5.24 (s, 1H, sugar hydroxyl), 5.17 (s, 2H, -CH_2-), 5.07 (d, 1H, *J* = 11.0 Hz, -CH_2-), 4.96 (d, 1H, *J* = 11.0 Hz, -CH_2-), 4.48 (d, 1H, *J* = 9.3 Hz, H-5″), 4.24 (m, 2H, -CH_2-), 3.73–3.51 (m, 4H, -CH_2- × 2), 3.45–3.42 (m, 3H, H-2″,3″,4″), 3.21 (t, 2H, -CH_2-), 2.47 (t, 2H, -CH_2-), 2.19 (m, 2H, -CH_2-). ^{13}C NMR (DMSO-d_6, 100 MHz) δ (ppm): 182.78, 165.80, 164.12, 162.02, 159.16, 156.41, 153.30, 152.60, 137.93, 137.71, 136.87, 136.52, 131.81, 130.42, 130.42, 128.93, 128.93, 128.85, 128.85, 128.62, 128.57, 128.57, 128.50, 128.50, 128.34, 128.34, 128.24, 127.78, 124.97, 123.31, 119.60, 115.81, 115.81, 110.07, 110.07, 106.26, 103.87, 99.33, 94.55, 76.39, 74.62, 73.18, 71.48, 70.49, 70.04, 68.79, 55.83, 53.35, 52.80, 45.43, 41.91.

*4.1.1.5. 3-(Phenylsulfonyl)-4-(2-(3,4,5-trihydroxy-6-((5-hydroxy-6-methoxy-2-(4-methoxyphenyl)-4-oxo-4H-chromen-7-yl)oxy)tetrahydro-2H-pyran-2-carboxamido)ethoxy)-1,2,5-oxadiazole-2-oxide (**15a**).*

Yellow power, 49.9 mg; yield: 13.2%, mp: 175–177 ^{o}C; MS(ESI) *m/z*: 758.1 $[M + H]^+$, 780.1 $[M + Na]^+$; HRMS (ESI) *m/z* calcd for $C_{33}H_{31}N_3NaO_{16}S$ $[M + Na]^+$ 780.1317, found 780.1315; ^{1}H NMR (DMSO-d_6, 400 MHz) δ (ppm): 12.92 (s, 1H, 5-OH), 8.24 (t, 1H, *J* = 5.4 Hz, -NH-), 8.02 (d, 2H, *J* = 9.0 Hz, H-2′,6′), 7.95 (d, 2H, *J* = 7.5 Hz, Ar-H), 7.82 (t, 1H, Ar-H), 7.69 (t, 2H, *J* = 7.5 Hz, Ar-H), 7.09 (d, 2H, *J* = 9.0 Hz, H-3′,5′), 7.04 (s, 1H, H-8), 6.93 (s, 1H, H-3), 5.59 (d, 1H, *J* =5.3 Hz, H-1″), 5.35 (d, 1H, *J* = 4.5 Hz, sugar hydroxyl), 5.30 (d, 1H, *J* = 4.5 Hz, sugar hydroxyl), 5.28 (brs, 1H, sugar hydroxyl), 4.43 (t, 2H, -CH_2-), 4.02 (d, 1H, *J* = 9.5 Hz, H-5″), 3.85 (s, 3H, -OCH_3), 3.76 (s, 3H, -OCH_3), 3.57–3.49 (m, 3H, H-2″,3″,4″), 3.40 (t, 2H, -CH_2-). ^{13}C NMR (DMSO-d_6, 100 MHz) δ (ppm): 182.81, 169.15, 164.36, 162.88, 159.19, 156.61, 153.07, 152.61, 137.36, 136.40, 133.05, 130.37, 130.37, 128.92, 128.92, 128.86, 128.86, 123.18, 115.00, 115.00, 111.07, 106.42, 103.82, 100.35, 94.66, 76.54, 76.27, 73.23, 71.67, 69.95, 60.78, 56.04, 37.81.

*4.1.1.6. 3-(Phenylsulfonyl)-4-(3-(3,4,5-trihydroxy-6-((5-hydroxy-6-methoxy-2-(4-methoxyphenyl)-4-oxo-4H-chromen-7-yl)oxy)tetrahydro-2H-pyran-2-carboxamido)propoxy)-1,2,5-oxadiazole-2-oxide (**15b**).*

Yellow power, 60.1 mg; yield: 15.6%, mp: 126–128 ^{o}C; MS(ESI) *m/z*: 772.1 $[M + H]^+$, 794.1 $[M + Na]^+$; HRMS (ESI) *m/z* calcd for $C_{34}H_{33}N_3NaO_{16}S$ $[M + Na]^+$ 794.1474, found 794.1457; ^{1}H NMR (DMSO-d_6, 400 MHz) δ (ppm): 12.96 (s, 1H, 5-OH), 8.36 (t, 1H, *J* = 5.2 Hz, -NH-), 8.05 (d, 2H, *J* = 8.9 Hz, H-2′,6′), 7.98 (d, 2H, *J* = 7.3 Hz, Ar-H), 7.84 (t, 1H, Ar-H), 7.69 (d, 2H, *J* = 7.5 Hz, Ar-H), 7.10 (d, 2H, *J* = 8.9 Hz, H-3′,5′), 7.06 (s, 1H, H-8), 6.95 (s, 1H, H-3), 5.70–5.51 (m, 4H, sugar hydroxyl), 4.35 (t, 2H, -CH_2-), 3.94 (d, 1H, *J* = 9.5 Hz, H-5″), 3.84 (s, 3H, -OCH_3), 3.73 (s, 3H, -OCH_3), 3.52–3.44 (m, 3H, H-2″,3″,4″), 3.26 (t, 2H, -CH_2-), 1.90 (t, 2H, -CH_2-). ^{13}C NMR (DMSO-d_6, 100 MHz) δ (ppm): 182.83, 169.15, 163.93, 162.76, 159.24, 155.59, 153.85, 152.72, 137.62, 136.55, 133.37, 130.48, 130.48, 128.82, 128.82, 128.06, 128.06, 122.14, 118.06,

118.06, 112.62, 106.18, 103.24, 100.53, 95.08, 76.75, 76.49, 74.39, 71.43, 69.45, 60.81, 56.05, 40.90.

*4.1.1.7. 3-(Phenylsulfonyl)-4-((1-(3,4,5-trihydroxy-6-((5-hydroxy-6-methoxy-2-(4-methoxyphenyl)-4-oxo-4H-chromen-7-yl)oxy)tetrahydro-2H-pyran-2-carboxamido)propan-2-yl)oxy)-1,2,5-oxadiazole-2-oxide (**15c**).*

Yellow power, 195.1 mg; yield: 50.6%, mp: 130–132 ^{o}C; MS(ESI) *m/z*: 772.1 $[M + H]^+$, 794.1 $[M + Na]^+$; HRMS (ESI) *m/z* calcd for $C_{34}H_{33}N_3NaO_{16}S$ $[M + Na]^+$ 794.1474, found 794.1458; ^{1}H NMR (DMSO-d_6, 400 MHz) δ (ppm): 12.92 (s, 1H, 5-OH), 8.23 (t, 1H, *J* = 5.6 Hz, -NH-), 8.05 (d, 2H, *J* = 8.9 Hz, H-2′,6′), 7.97 (d, 2H, *J* = 7.5 Hz, Ar-H), 7.83 (t, 1H, Ar-H), 7.69 (d, 2H, *J* = 7.5 Hz, Ar-H), 7.09 (d, 2H, *J* = 8.9 Hz, H-3′,5′), 7.03 (s, 1H, H-8), 6.95 (s, 1H, H-3), 5.60 (brs, 1H, H-1″), 5.35–5.51 (m, 3H, sugar hydroxyl), 4.97 (m, 1H, -CH-), 4.01 (d, 1H, *J* = 9.3 Hz, H-5″), 3.86 (s, 3H, $-OCH_3$), 3.75 (s, 3H, $-OCH_3$), 3.59–3.50 (m, 3H, H-2″,3″,4″), 3.42(d, 2H, $-CH_2-$), 1.28 (d, 3H, $-CH_3$). ^{13}C NMR (DMSO-d_6, 100 MHz) δ (ppm): 182.83, 168.99, 164.32, 162.90, 158.67, 156.61, 153.06, 152.59, 137.41, 136.41, 133.05, 130.31, 130.31, 129.06, 129.06, 128.84, 128.84, 123.14, 119.55, 119.55, 111.13, 106.45, 103.80, 100.47, 94.65, 78.03, 76.72, 73.24, 71.54, 71.34, 60.79, 56.04, 17.26.

*4.1.1.8. 3-(Phenylsulfonyl)-4-(2-(4-(3,4,5-trihydroxy-6-((5-hydroxy-6-methoxy-2-(4-methoxyphenyl)-4-oxo-4H-chromen-7-yl)oxy)tetrahydro-2H-pyran-2-carbonyl)piperazin-1-yl)ethoxy)-1,2,5-oxadiazole-2-oxide. (**15d**).*

Yellow power, yield: 10.9%, mp: 119–121 ^{o}C; MS(ESI) *m/z*: 827.1 $[M + H]^+$, 849.1 $[M + Na]^+$; HRMS (ESI) *m/z* calcd for $C_{37}H_{38}N_4NaO_{16}S$ $[M + Na]^+$ 849.1896, found 849.1879; ^{1}H NMR (DMSO-d_6, 400 MHz) δ (ppm): 12.90 (s, 1H, 5-OH), 8.01 (d, 2H, *J* = 8.9 Hz, H-2′,6′), 7.95 (d, 2H, *J* = 8.1 Hz, Ar-H), 7.85 (t, 1H, Ar-H), 7.70 (d, 2H, *J* = 8.1 Hz, Ar-H), 7.17 (s, 1H, H-8), 7.06 (d, 2H, *J* = 8.9 Hz, H-3′,5′), 6.94 (s, 1H, H-3), 5.61 (d, 1H, *J* = 4.0 Hz, H-1″), 5.45 (d, 1H, *J* = 7.2 Hz, sugar hydroxyl), 5.22–5.17 (m, 3H, sugar hydroxyl), 4.48 (d, 1H, *J* = 9.4 Hz, H-5″), 4.24 (m, 2H, $-CH_2-$), 3.82 (s, 3H, $-OCH_3$), 3.75 (s, 3H, $-OCH_3$), 3.68–3.53 (m, 4H, $-CH_2-$ × 2),

3.43–3.37 (m, 3H, H-2″,3″,4″), 3.22 (t, 2H, -CH_2-), 2.47 (m, 2H, -CH_2-), 2.23 (m, 2H, -CH_2-). ^{13}C NMR (DMSO-d_6, 100 MHz) δ (ppm): 182.80, 165.81, 164.17, 162.93, 159.16, 156.28, 153.05, 152.51, 137.71, 136.54, 133.01, 130.44, 130.44, 128.63, 128.63, 127.78, 127.78, 124.96, 119.60, 119.60, 110.08, 106.30, 103.80, 99.40, 94.60, 76.32, 73.05, 71.37, 70.50, 68.82, 60.77, 56.04, 55.08, 53.38, 52.87, 45.46, 41.93.

*4.1.2. General procedure for the synthesis of compounds **16a, 16b, 17a** and **17b***

To a solution of **12** or **13** (0.5 mmol) and DBU (0.6 mmol) in DMF (5 mL) **9a** or **9b** (0.6 mmol) was added. The mixture was stirred at room temperature for 3 h. Then, the mixture was poured into 20 mL of H_2O, and extracted with EtOAc (3 × 20 mL). The organic layer was combined, washed with brine, dried over anhydrous Na_2SO_4, and concentrated in vacuo. The crude product was purified by silica gel column chromatography eluting with dichloromethane/methanol system.

*4.1.2.1. 2-(Nitrate)ethyl-6-((6-(benzyloxy)-2-(4-(benzyloxy)phenyl)-5-hydroxy-4-oxo -4H-chromen-7-yl)oxy)-3,4,5-trihydroxytetrahydro-2H-pyran-2-carboxylate (**16a**).*

Yellow power, 142 mg; yield: 38.8%, mp: 156–158 ^{o}C; MS(ESI) *m/z*: 732.2 $[M + H]^+$, 754.1 $[M + Na]^+$; HRMS (ESI) *m/z* calcd for $C_{37}H_{33}NNaO_{15}$ $[M + Na]^+$ 754.1742, found 754.1739; ^{1}H NMR (DMSO-d_6, 400 MHz) δ (ppm): 12.97 (s, 1H, 5-OH), 8.05 (d, 2H, *J* = 8.9 Hz, H-2′,6′), 7.55 (d, 2H, *J* = 7.4 Hz, Ar-H), 7.48 (d, 2H, *J* = 7.4 Hz, Ar-H), 7.42–7.31 (m, 6H, Ar-H), 7.21 (d, 2H, *J* = 8.9 Hz, H-3′,5′), 7.12 (s, 1H, H-8), 6.95 (s, 1H, H-3), 5.71 (d, 1H, *J* =5.1 Hz, H-1″), 5.54 (d, 1H, *J* =5.8 Hz, sugar hydroxyl), 5.42 (d, 1H, *J* =7.8 Hz, sugar hydroxyl), 5.41 (brs, 1H, sugar hydroxyl), 5.22 (s, 2H, -CH_2-), 5.09 (d, 1H, *J* =10.8 Hz, -CH_2-), 4.96 (d, 1H, *J* =10.8 Hz, -CH_2-), 4.22 (d, 1H, *J* = 9.6 Hz, H-5″), 4.14–4.09 (m, 2H, -CH_2-), 3.50–3.47 (m, 3H, H-2″,3″,4″), 3.44 (t, 2H, -CH_2-). ^{13}C NMR (DMSO-d_6, 100 MHz) δ (ppm): 182.84, 169.00, 164.32, 162.00, 156.58, 153.31, 152.70, 137.98, 136.91, 131.78, 128.98, 128.98, 128.86, 128.86, 128.58, 128.58, 128.52, 128.52, 128.34, 128.34, 123.40, 115.87, 115.87, 106.40, 103.94, 99.80, 94.42, 76.14, 75.61, 74.66, 73.38, 71.72, 71.72, 70.05, 61.38.

*4.1.2.2. 3-(Nitrate)propyl-6-((6-(benzyloxy)-2-(4-(benzyloxy)phenyl)-5-hydroxy-4-oxo-4H-chromen-7-yl)oxy)-3,4,5-trihydroxytetrahydro-2H-pyran-2-carboxylate (**16b**).*

Yellow power, 295 mg; yield: 79.2%, mp: 106–108 ^{o}C; MS(ESI) *m/z*: 746.1 $[M + H]^+$, 768.1 $[M + Na]^+$; ^{1}H NMR (DMSO-d_6, 400 MHz) δ (ppm): 12.97 (s, 1H, 5-OH), 8.03 (d, 2H, J = 8.6 Hz, H-2′,6′), 7.56 (d, 2H, J = 7.3 Hz, Ar-H), 7.47 (d, 2H, J = 7.3 Hz, Ar-H), 7.42–7.32 (m, 6H, Ar-H), 7.20 (d, 2H, J = 8.6 Hz, H-3′,5′), 7.12 (s, 1H, H-8), 6.93 (s, 1H, H-3), 5.71 (d, 1H, J = 5.4 Hz, H-1″), 5.59 (d, 1H, J = 5.8 Hz, sugar hydroxyl), 5.43 (d, 2H, J = 7.6 Hz, sugar hydroxyl), 5.21 (s, 2H, -CH_2-), 5.09 (d, 1H, J =10.9 Hz, -CH_2-), 4.96 (d, 1H, J =10.9 Hz, -CH_2-), 4.54 (t, 2H, -CH_2-), 4.25 (d, 1H, J = 9.7 Hz, H-5″), 4.18 (t, 2H, -CH_2-), 3.51–3.47 (m, 3H, H-2″, 3″,4″), 2.02–1.98 (m, 2H, -CH_2-). ^{13}C NMR (DMSO-d_6, 100 MHz) δ (ppm): 182.80, 169.08, 164.30, 162.00, 156.57, 153.33, 152.69, 138.01, 136.91, 131.85, 128.95, 128.95, 128.84, 128.84, 128.56, 128.56, 128.49, 128.49, 128.28, 128.28, 123.39, 115.84, 115.84, 106.42, 103.91, 99.95, 94.47, 76.28, 75.73, 74.67, 73.44, 71.77, 70.07, 66.72, 61.47, 26.00. HRMS (ESI) *m/z* calcd for $C_{38}H_{35}NNaO_{15}$ $[M + Na]^+$ 768.1899, found 768.1853.

*4.1.2.3. 2-(Nitrate)ethyl-3,4,5-trihydroxy-6-((5-hydroxy-6-methoxy-2-(4-methoxyphenyl)-4-oxo-4H-chromen-7-yl)oxy)tetrahydro-2H-pyran-2-carboxylate (**17a**).*

Yellow power, 202 mg; yield: 69.8%, mp: 149–151 ^{o}C; MS(ESI) *m/z*: 580.1 $[M + H]^+$, 602.1 $[M + Na]^+$; HRMS (ESI) *m/z* calcd for $C_{25}H_{26}NO_{15}$ $[M + H]^+$ 602.1116, found 602.1119; ^{1}H NMR (DMSO-d_6, 400 MHz) δ (ppm): 12.94 (s, 1H, 5-OH), 8.06 (d, 2H, J = 8.9 Hz, H-2′,6′), 7.12 (d, 2H, J = 8.9 Hz, H-3′,5′), 7.08 (s, 1H, H-8), 6.97 (s, 1H, H-3), 5.65 (d, 1H, J =5.0 Hz, H-1″), 5.56 (d, 1H, J =5.6 Hz, sugar hydroxyl), 5.39–5.36 (m, 2H, sugar hydroxyl), 4.75 (t, 2H, -CH_2-), 4.41 (m, 2H, -CH_2-), 4.25 (d, 1H, J = 9.4 Hz, H-5″), 3.86 (s, 3H, -OCH_3), 3.76 (s, 3H, -OCH_3), 3.47–3.40 (m, 3H, H-2″,3″,4″). ^{13}C NMR (DMSO-d_6, 100 MHz) δ (ppm): 182.85, 169.00, 164.39, 162.94, 156.47, 153.09, 152.61, 133.03, 128.85, 128.85, 123.20, 115.07, 115.07, 106.45, 103.88, 99.96, 94.57, 76.06, 75.58, 73.26, 71.74, 71.74, 61.38, 60.79, 56.07.

*4.1.2.4. 3-(Nitrate)propyl-3,4,5-trihydroxy-6-((5-hydroxy-6-methoxy-2-(4-methoxyphenyl)-4-oxo-4H-chromen-7-yl)oxy)tetrahydro-2H-pyran-2-carboxylate (**17b**).*

Yellow power, 50.1 mg; yield: 16.9%, mp: 105–107 ^{o}C; MS(ESI) *m/z*: 594.0 $[M + H]^+$, 615.9 $[M + Na]^+$; HRMS (ESI) *m/z* calcd for $C_{26}H_{28}NO_{15}$ $[M + H]^+$ 594.1453, found 594.1483; ^{1}H NMR (DMSO-d_6, 400 MHz) δ (ppm): 12.93 (s, 1H, 5-OH), 8.04 (d, 2H, J = 8.9 Hz, H-2′,6′), 7.13 (d, 2H, J = 8.9 Hz, H-3′,5′), 7.07 (s, 1H, H-8), 6.94 (s, 1H, H-3), 5.62 (d, 1H, J =5.1 Hz, H-1″), 5.54 (d, 1H, J =5.7 Hz, sugar hydroxyl), 5.36–5.34 (m, 2H, sugar hydroxyl), 4.55 (t, 2H, -CH_2-), 4.21 (d, 1H, J = 9.7 Hz, H-5″), 4.17 (t, 2H, -CH_2-), 3.86 (s, 3H, -OCH_3), 3.77 (s, 3H, -OCH_3), 3.47–3.38 (m, 3H, H-2″,3″,4″), 2.01 (m, 2H, -CH_2-). ^{13}C NMR (DMSO-d_6, 100 MHz) δ (ppm): 182.83, 169.07, 164.38, 162.94, 156.44, 153.09, 152.60, 133.06, 128.82, 128.82, 123.21, 115.07, 115.07, 106.45, 103.87, 100.03, 94.56, 76.18, 75.68, 73.30, 71.72, 70.87, 61.45, 60.77, 56.06, 26.00.

4.2. MTT assay

Cytotoxicity of all the tested compounds against MCF-7, HCT-116, PC-3, and HepG2 cells was determined by MTT assay. Cells were planted into 96-well micro-plates at a density of 2.0-4.0 × 10^4 cells/mL (100 μL per well). After overnight incubation at 37 ^{o}C, 5-9 different concentrations of test compounds were added to the wells. Compounds were dissolved in DMSO before being diluted in the growth medium. The concentration of DMSO in the wells did not exceed 0.5%. Cells were further incubated for 72 h, at the end of the incubation time, fresh medium containing 0.5 mg/mL of MTT were added. Plates were incubated for another 4 h at 37 ^{o}C, the media was removed and formazan crystals formed in the cells were dissolved in 200 μL of DMSO. Optical density was measured at 570 nm with DMSO as blank using a Bio-Rad microplate reader (Model 680). In these experiments, the negative reference was 0.1% DMSO, scutellarin and 5-FU were used as the positive references.

4.3. NO releasing test

The levels of NO generated by individual compounds were determined by the colorimetric assay using the nitrite colorimetric assay kit (Beyotime, China), according to the manufacturer's instructions. Incubation in phosphate buffer solution (pH 7.4) containing 2% dimethyl sulfoxide and 10^{-5} M of the test compound (1 mL of 0.2 mM solution in 0.1 M phosphate buffer, pH 7.4) was mixed with a freshly prepared solution of L-cysteine (1 mL of a 3.6 mM solution in 0.1 M phosphate buffer, pH 7.4) at 37 ^{o}C for 1 h, 2h and 3h in the absence of air. After exposure to air for 10 min at 25 ^{o}C, an aliquot of the Griess reagent I (50 μL) and Griess reagent II (50 μL) was added to an equal volume (50 μL) of each test compound's incubation solution. After 10 min, the absorbance was measured at 540 nm. Solutions of 1 M sodium nitrite were used to prepare a nitrite absorbance *versus* concentration curve under the same experimental conditions. The different concentrations of nitrite were used as standards to calculate the concentrations of NO formed by individual test compound.

Intracellular NO release data were acquired using the Griess reaction in HepG2 and L-O2 cells according to the manufacturer's instructions (S0024, Beyotime, China). Briefly, cells were treated with 100 μM of each compound for 2.5 h. Subsequently, the cells were harvested and their cell lysates were prepared and then mixed with Griess reagent for 10 min at 37 ^{o}C, followed by measurement at 540 nm by a microplate reader. The cells treated with 0.4% DMSO in medium were used as negative control for the background levels of nitrite production, while sodium nitrite at different concentrations was prepared as the positive control for the establishment of a standard curve.

4.4. Cell cycle study

The cell were incubated with different concentrations of the test compounds **14b** and **15a** or vehicle as described above. After incubation for 72 h, the treated cells were trypsinized, washed with PBS and centrifuged at 2000 rpm/min. The collected cells were fixed by adding cold ethanol (4 ^{o}C overnight) and incubated for 30 min in PBS containing 100 μL RNase A of RNase and 400

μL of PI. Cell DNA content was measured using flow cytometry (FACS Calibur Bectone-Dickinson) for cell cycle distribution analysis.

4.5. Hoechst 333258 staining

Cells grown on a sterile cover slip in 6-well plates were treated with test compounds **14b** and **15a** or vehicle for a certain range of time. The culture medium containing compounds was removed, and the cells were fixed in 4% paraformaldehyde for 10 min. After being washed twice with PBS, the cells were stained with 0.5 mL of Hoechst 33258 (Keygen, Nanjing, China) for 5 min and then again washed twice with PBS. The stained nuclei were observed under a flow cytometry (FACS Calibur Bectone-Dickinson) using 350 nm excitation and 460 nm emission.

4.6. Analysis of cellular apoptosis

Cells were seed into 6-well plates and incubated for 24 h at 37 ^{o}C under an atomosphere of 5% CO_2. Then test compounds **14b** and **15a** were added in a certain concentration and the negative control which was treated with DMSO were included. After incubation for 72 h, the treated cells were trypsinized, then washed with PBS twice and centrifuged at 2000 rpm to collect the cells (5 $\times$ 10^5). After 500 μL of binding buffer was added to suspend the cells, 5 μL of Annexin V-APC and 7-AAD or PI were added successively and mixed well. Followed by 5–15 min incubation at room temperature in dark, cell apoptosis was analyzed with flow cytometry (FACS Calibur Bectone-Dickinson).

4.7. Cell mitochondrial membrane potential assay

Cells were cultured overnight and incubated in triplicate with the test compounds **14b** and **15a** or vehicle for 48 h. The cells were stained with the lipophilic cationic dye JC-1, according to the manufacturer's instruction (Keygen, KGA601). The percentage of cells with healthy or collapsed

mitochondrial membrane potentials was monitored by flow cytometry analysis.

4.8. Quantitation of cellular proteins involved in apoptosis

The relative expression levels of 35 apoptosis-related proteins were evaluated using Human Apoptosis Array kit (R&D Systems, Abingdon, UK) in HepG2 cells. Proteins were extracted according to the manufacturer's protocol from cells treated for 24 h with compound **14b** (2 μM).

Acknowledgment

This work was financially supported by the Key Laboratory for the Chemistry and Molecular Engineering of Medicinal Resources (Guangxi Normal University), the Ministry of the Education of China (CMEMR2015-B07).

References

[1] T. Rodrigues, D. Reker, P. Schneider, G. Schneider, Nat. Chem. 8 (2016) 531–541.
[2] B.B. Mishra, V.K. Tiwari, Eur. J. Med. Chem. 46 (2011) 4769–4807.
[3] D.J. Newman, G.M. Cragg, J. Nat. Prod. 79 (2016) 629–661.
[4] M. Singh, M. Kaur, O. Silakari, Eur. J. Med. Chem. 84 (2014) 206–239.
[5] M. Li-Weber, Cancer Lett. 332 (2013) 304–312.
[6] B. Almeida Rezende, A.C. Pereira, S.F. Cortes, V.S. Lemos, Curr. Med. Chem. 23 (2016) 87–102.
[7] K. Gasiorowski, E. Lamer-Zarawska, J. Leszek, K. Parvathaneni, B.B. Yendluri, Z. Błach-Olszewska, G. Aliev, CNS Neurol. Disord. Drug Targets 10 (2011) 184–191.
[8] Z.X. Gao, D.Y. Huang, H.X. Li, L.N. Zhang, Y.H. Lv, H.D. Cui, J.H. Zheng, Biochem. Biophys. Res. Commun. 400 (2010) 151–156
[9] M. Li-Weber, Cancer Treat. Rev. 35 (2009) 57–68.
[10] Z.H. Shi, N.G. Li, Z.J. Wang, Y.P. Tang, Z.X. Dong, W. Zhang, P.X. Zhang, T. Gu, W.Y. Wu, J.P. Yang, J.A. Duan, Eur. J. Med. Chem. 106 (2015) 95–105.
[11] X.Y. Chen, X.G. Shi, X. Zhang, H.X. Lei, S.M. Long, H.X. Su, Z. Pei, R.X. Huang, Mediators Inflamm. 2013 (2013).
[12] Z.W. Pan, W.M. Zhao, X.Y. Zhang, B. Wang, J.H. Wang, X.L. Sun, X.T. Liu, S.Y. Feng, B.F. Yang, Y.J. Lu, Br. J. Pharmacol. 162 (2011) 688–700.

[13] H. Zhou, X. Chen, L.Z. Chen, X. Zhou, G.S. Zheng, H.Q. Zhang, W.J. Huang, J.J. Cai, Molecules 19 (2014) 15611−15623.

[14] Z. Wang, J.G. Yu, J.B. Wu, F. Qi, H.L. Wang, Z.G. Wang, Z.J. Xu, Life Sci. 157 (2016) 200−207.

[15] L.H. Qian, M.Z. Shen, H. Tang, Y.P. Tang, L. Zhang, Y.F. Fu, Q.P. Shi, N.G. Li, Molecules 17 (2012) 10667−10674.

[16] Y.Z. Feng, S.S. Zhang, J. Tu, Z.F. Cao, Y.Y. Pan, B.X. Shang, R.F. Liu, M.M. Bao, P.D. Guo, Q.S. Zhou, Leuk. Lymphoma 53 (2012) 2456−2464.

[17] C.Z. Wang, X.L. Li, Q.F. Wang, S.R. Mehendale, C.S. Yuan, Phytomedicine 17 (2010) 63−68.

[18] H.T. Xu, S.Y. Zhang, Phytother. Res. 27 (2013) 1524−1528.

[19] Y. Ke, T.H. Bao, X.S. Wu, H.R. Tang, Y. Wang, J.Y. Ge, B.M. Fu, X. Meng, L. Chen, C. Zhang, Y.Q. Tan, H.T. Chen, Z.T. Guo, F. Ni, X.F. Lei, Z.T. Shi, D. Wei, L. Wang, Biochem. Biophys. Res. Commun. (2016) http://dx.doi.org/10.1016/j.bbrc.2016.12.114.

[20] H.X. Li, D.Y. Huang, Z.X.Z. Gao, Y.H. Lv, L.N. Zhang, H.D. Cui, J.H. Zheng, Oncol. Rep. 24 (2010) 1153−1160.

[21] H.X. Li, D.Y. Huang, Z.X.Z. Gao, Y. Chen, L.N. Zhang, J.H. Zheng, Int. J. Oncol. 42 (2013) 1674−1681.

[22] H.X. Li, H.X. Fan, Z. Wang, J.H. Zheng, W.W. Cao, Plos One 8 (2013) e59473.

[23] N.G. Li, M.Z. Shen, Z.J. Wang, Y.P. Tang, Z.H. Shi, Y.F. Fu, Q.P. Shi, H. Tang, J.A. Duan, Bioorg. Med. Chem. Lett. 23 (2013) 102−106.

[24] D.R. Ding, B.Z. Zhang, T. Meng, Y. Ma, X. Wang, H.L. Peng, J.K. Shen, Org. Biomol. Chem. 9 (2011) 7287−7291.

[25] R. Luo, J.B. Wang, L. Zhao, N. Lu, Q.D. You, Q.L. Guo, Z.Y. Li, Bioorg. Med. Chem. Lett. 24 (2014) 1334–1338.

[26] Q.L. Song, S.W. Tan, X.T. Zhuang, Y.Y. Guo, Y.D. Zhao, T.T. Wu, Q. Ye, L.Q. Si, Z.P. Zhang, Mol. Pharm. 11 (2014) 4118–4129.

[27] R.A. Serafim, M.C. Primi, G.H. Trossini, E.I. Ferreira, Curr. Med. Chem. 19 (2012) 386−405.

[28] C. Szabo, Nat. Rev. Drug Discov. 15 (2016) 185−203.

[29] B. Bonavida, H. Garban, Redox Bio. 6 (2015) 486−494.

[30] A.W. Carpenter, M.H. Schoenfisch, Chem. Soc. Rev. 41 (2012) 3742−3752.

[31] H. Cerecetto, W. Porcal, Mini. Rev. Med. Chem. 5 (2005) 57−71.

[32] Z.G. Ren, X.K. Gu, B. Lu, Y.Q. Chen, G.J. Chen, J.N. Feng, J.Z. Lin, Y.H. Zhang, H. Peng, J. Cell Mol. Med. 20 (2016) 1095−1105.

[33] M.M. Liu, X.Y. Chen, Y.Q. Huang, P. Feng, Y.L. Guo, G. Yang, Y. Chen, J. Med. Chem. 57 (2014) 9343−9356.

[34] Y. Ai, F.H. Kang, Z.J. Huang, X.W. Xue, Y.S. Lai, S.X. Peng, J.D Tian, Y.H. Zhang, J. Med. Chem. 58 (2015) 2452−2464.

[35] L. Fang, M. Wang, S.H. Gou, X.Y. Liu, H. Zhang, F. Cao, J. Med. Chem. 57 (2014) 1116−1120.

[36] S. Huerta, S. Chilka, B. Bonavida, Int. J. Oncol. 33 (2008) 909–927.
[37] Q.Q Wang, N. Cheng, W.B. Yi, S.M. Peng, X.Q. Zou, Bioorg. Med. Chem. 22 (2014) 1515–1521.
[38] Q.Q Wang, N. Cheng, X.W. Zheng, S.M. Peng, X.Q. Zou, Bioorg. Med. Chem. 21 (2013) 4301–4310.
[39] M.A.E. Mourad, M. Abdel-Aziz, G.A.A. Abuo-Rahma, H.H. Farag, Eur. J. Med. Chem. 54 (2012) 907–913.
[40] Y. Ling, X.L. Ye, Z.Z. Zhang, Y.H. Zhang, Y.S. Lai, H. Ji, S.X. Peng, J.D. Tian, J. Med. Chem. 54 (2011) 3251–3259.
[41] Y.C. Zhang, J.Y. Xu, Y.M. Li, H.Q. Yao, X.M. Wu, Chem. Biol. Drug Des. 85 (2015) 541–548.
[42] B.M.F. Gonçalves, J.A.R. Salvador, S. Marín, M. Cascante, Eur. J. Med. Chem. 114 (2016) 101–117.
[43] B. Bonavida, S. Baritaki, S. Huerta-Yepez, M.I. Vega, D. Chatterjee, K. Yeung, Nitric Oxide 19 (2008) 152–157.
[44] D.R. Green, J.C. Reed, Science 281 (1998) 1309–1312.
[45] H. Liu, Q. Li, Y. Wang, H.M. Hong, M.T. Chen, Y.Y. Wang, F.F. Hong, S.L. Yang, Hepatol. Res. (2016) http://dx.doi.org/10.1111/hepr.12783.
[46] J.F.R. Kerr, A.H. Wyllie, A.R. Currie, Br. J. Cancer 26 (1972) 239–257.
[47] G.M. Cohen, Biochem. J. 326 (1997) 1–16.
[48] D.C. Altieri, Biochem. J. 430 (2010) 199–205.
[49] X.M. Xu, M.L. Zhang, Y. Zhang, L. Zhao, Oncol. Lett. 12 (2016) 3779–3784.
[50] S.K. Calderwood, J.L. Gong, Trends Biochem. SCI. 41 (2016) 311–323.
[51] F.J. Quintana, I.R. Cohen, Trends Immunol. 32 (2011) 89–95.
[52] S. Kumar, J. Stokes III, U.P. Singh, K.S. Gunn, A. Acharya, U. Manne, M. Mishra, Cancer Lett. 374 (2016) 156–166.
[53] C. Wang, Y.R. Zhang, K. Guo, N. Wang, H.J. Jin, Y.K. Liu, W.X. Qin, Int. J. Cancer 138 (2016) 1824–1834.
[54] M. Shevtsov, G. Multhoff, Front. Immuno. 7 (2016) 171.
[55] L. Salerno, V. Pittala, G. Romeo, M.N. Modica, A. Marrazzo, M.A. Siracusa, V. Sorrenti, C.D. Giacomo, L. Vanella, N.N. Parayath, K. Greish, Eur. J. Med. Chem. 96 (2015) 162–172.
[56] L.Y. Chau, J. Biomed. Sci. 22 (2015) 22.
[57] P.A. Dennery, Antioxid. Redox Sign. 20 (2014) 1743–1753.

Table 1

Effects of the compounds on cell viability against different cell lines.

Compound	IC_{50} (μM)[a]					
	MCF-7	HCT-116	PC-3	HepG-2	L-O2	SI[b]
14a	2.51 ± 0.34	13.58 ± 0.47	0.36 ± 0.03	1.48 ± 0.15	19.31 ± 0.86	13.0
14b	2.96 ± 0.21	7.25 ± 1.38	0.09 ± 0.01	0.50 ± 0.07	47.96 ± 1.24	95.9
14c	1.99 ± 0.99	2.59 ± 0.82	0.74 ± 0.31	1.83 ± 0.59	32.46 ± 1.10	17.7
14d	1.65 ± 0.78	5.70 ± 3.63	0.67 ± 0.12	6.40 ± 0.66	39.87 ± 1.75	6.2
15a	39.97 ± 1.89	1.74 ± 0.38	1.45 ± 0.53	10.88 ± 1.32	34.49 ± 1.22	3.2
15b	21.71 ± 0.93	2.46 ± 0.57	3.10 ± 0.46	12.35 ± 0.83	45.90 ± 2.37	3.7
15c	8.25 ± 0.77	2.16 ± 1.26	3.01 ± 0.89	12.92 ± 1.41	41.58 ± 1.84	3.2
15d	3.64 ± 0.86	1.27 ± 0.32	3.65 ± 0.81	9.53 ± 0.72	22.94 ± 0.56	2.4
16a	> 50	> 50	> 50	> 50	NT[c]	
16b	30.83 ± 4.79	17.40 ± 1.7	18.79 ± 1.34	36.75 ± 2.23	NT	
17a	> 50	> 50	> 50	> 50	NT	
17b	> 50	> 50	> 50	> 50	NT	
Scutellarin	> 100	77 ± 2.35	72.90 ± 1.37	56.09 ± 1.23	> 100	
5-FU	28.73 ± 3.94	4.16 ± 0.23	24.33 ± 0.36	29.07 ± 0.93	NT	

[a] IC_{50}: Half inhibitory concentrations measured by the MTT assay. The values are expressed as average ± standard deviations of three independent experiments. [b] SI: selectivity index. It was calculated as: SI = $IC_{50,}$ L-O2/HepG-2. [c] NT: not tested.

Table 2

The amount of NO released by the tested compounds

Compound	The amounts of released-NO (μmol/L)					
	0.25 h	0.5 h	0.75 h	1 h	2 h	3 h
14a	11.20	14.27	17.53	19.52	26.39	39.95
14b	7.58	10.11	11.92	13.55	16.26	20.06
14c	11.92	13.91	15.72	17.71	19.33	18.97
14d	7.94	11.74	12.64	14.27	21.87	23.86
15a	26.93	33.26	41.94	49.35	58.03	59.12
15b	11.74	15.54	20.42	24.22	30.55	30.37
15c	12.46	20.78	24.94	34.16	46.46	44.29
15d	13.73	20.78	26.03	33.80	37.96	39.41
16a	3.96	4.51	4.69	6.13	4.87	5.05
16b	4.14	4.33	4.69	5.05	3.78	3.24
17a	1.07	1.97	2.34	2.34	1.97	1.79
17b	0.53	1.25	1.61	1.25	1.43	1.25

1. Legends for Fig. 1, Fig. 2, Fig. 3, Fig. 4, Fig. 5, Fig. 6 , Fig. 7, Scheme 1 and Scheme 2

Fig. 1. The chemical structures of reported natural product/nitric oxide donor hybrids (**18**–**21**).

Fig. 2. The NO level in HepG2 and L-O2 cells.

Fig. 3. Cell cycle analysis of compounds **14b** (A) in HepG2 and **15a** (B) in PC-3 cells by flow cytometry.

Fig. 4. Hoechst staining of compounds **14b** (A) in HepG2 and **15a** (B) in PC-3 cells.

Fig. 5. Flow cytometry analysis of compounds **14b** (A) induced apoptosis in HepG2, **15a** (B) in PC-3 cells and the apoptosis of nontumor LO-2 cells induced by **14b** and **15a** (C).

Fig. 6. 14b (A) induced mitochondrial depolarization in HepG2 and **15a** (B) in PC-3 cells.

Fig. 7. The effects exerted by compound **14b** on the expression of apoptosis-related proteins using the Human Apoptosis Array kit in HepG2 cells.

Scheme 1. Synthesis of compounds (**6a-d**) and (**9a**, **b**). Reagents and conditions: (a) $ClCH_2COOH$, NaOH (aq), reflux, 2 h; (b) 30% H_2O_2, AcOH, rt, 3 h; (c) fuming HNO_3, 90 ^oC, 4 h; (d) aminoalcohol, THF, NaH,0 °C, 4 h; (e) fuming HNO_3, H_2SO_4, 0 ^oC, 3 h.

Scheme 2. Synthesis of compounds (**14a-d**), (**15a-d**), (**16a**, **b**) and (**17a**, **b**). Reagents and conditions: (a) BnBr or CH_3I, K_2CO_3, DMF, rt, 24 h; (b) KOH, MeOH/DCM, rt, 2-3 h; (c) **6a-d**, HOBt, EDCI, DMF, rt, 3 h; (d) **9a**, **b**, DBU, DMF, rt, 2 h.

2. Graphics for Fig. 1, Fig. 2, Fig. 3, Fig. 4, Fig. 5, Fig. 6 , Fig. 7, Scheme 1 and Scheme 2

Figure 1

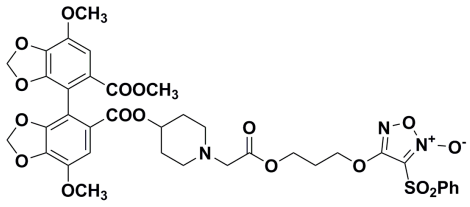

18

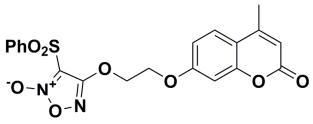

19

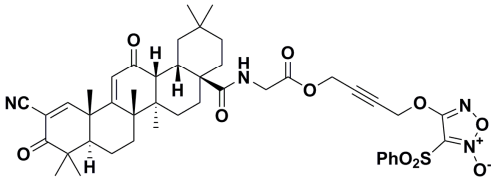

20

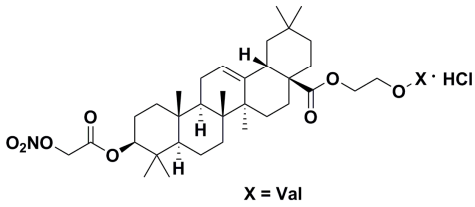

21

Figure 2

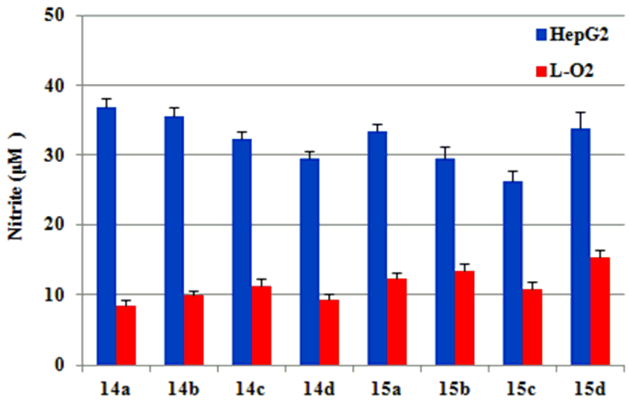

Figure 3

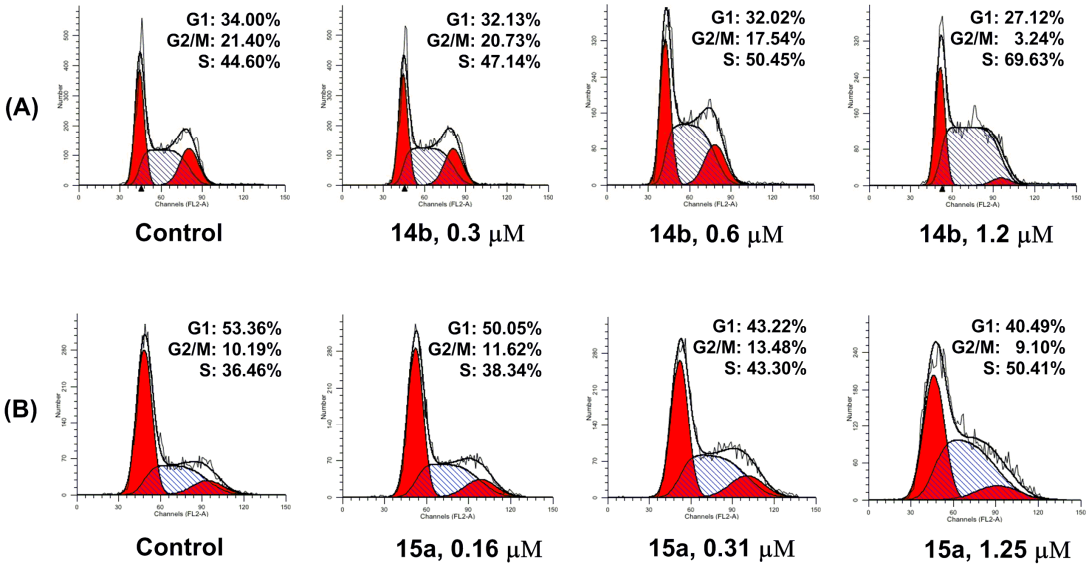

Figure 4

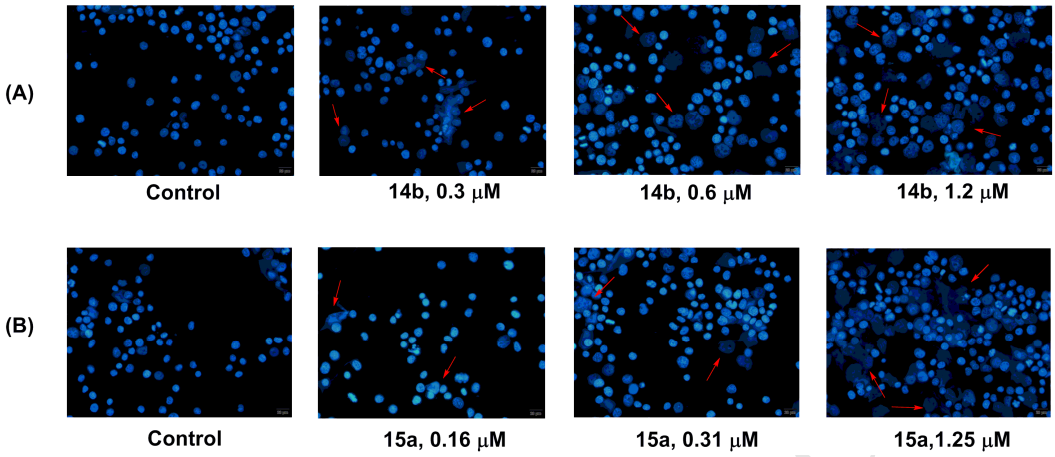

Figure 5

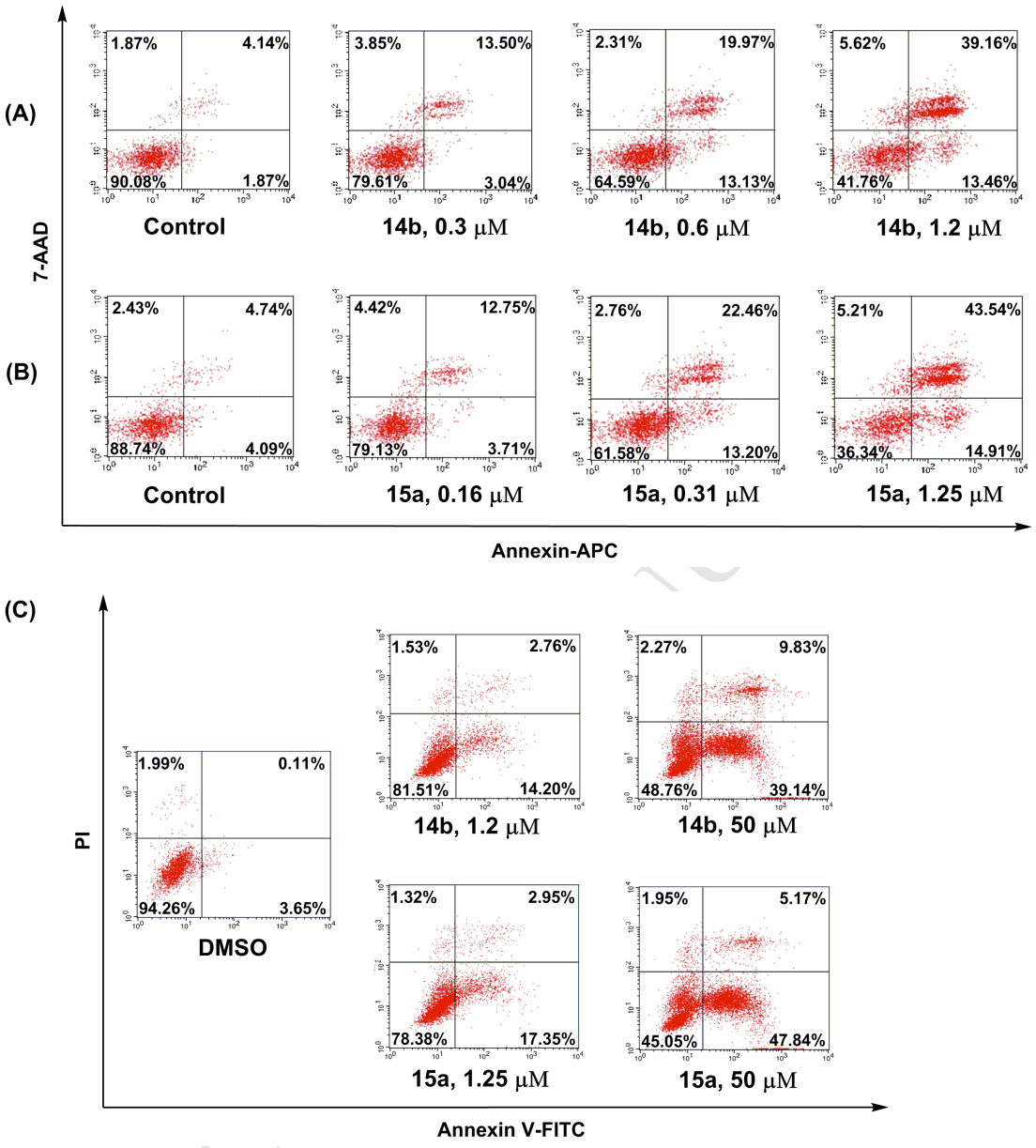
(A)
(B)
7-AAD
1.87%
4.14%
90.08%
1.87%
Control
3.85%
13.50%
79.61%
3.04%
14b, 0.3 μM
2.31%
19.97%
64.59%
13.13%
14b, 0.6 μM
5.62%
39.16%
41.76%
13.46%
14b, 1.2 μM
2.43%
4.74%
88.74%
4.09%
Control
4.42%
12.75%
79.13%
3.71%
15a, 0.16 μM
2.76%
22.46%
61.58%
13.20%
15a, 0.31 μM
5.21%
43.54%
36.34%
14.91%
15a, 1.25 μM
Annexin-APC
(C)
PI
1.99%
0.11%
94.26%
3.65%
DMSO
1.53%
2.76%
81.51%
14.20%
14b, 1.2 μM
2.27%
9.83%
48.76%
39.14%
14b, 50 μM
1.32%
2.95%
78.38%
17.35%
15a, 1.25 μM
1.95%
5.17%
45.05%
47.84%
15a, 50 μM
Annexin V-FITC

Figure 6

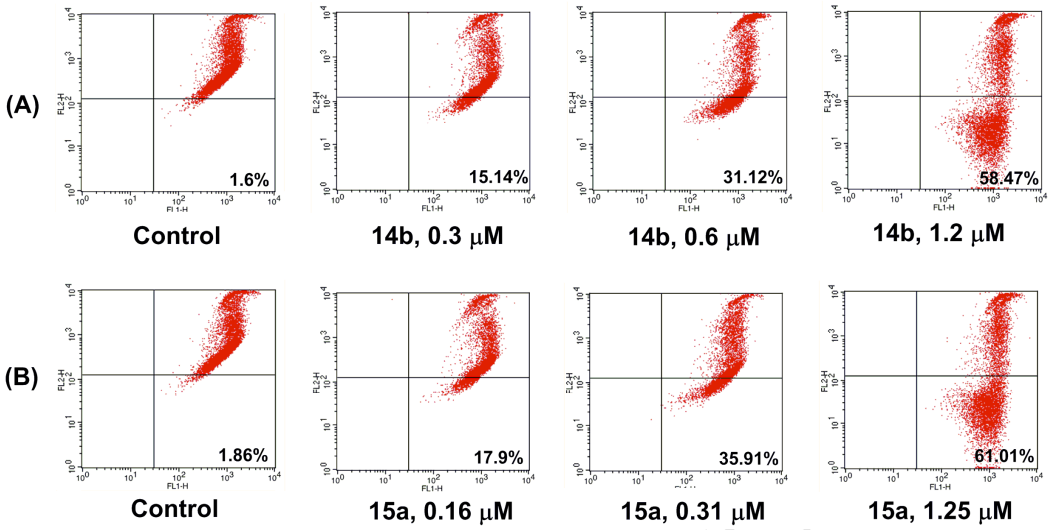

Figure 7

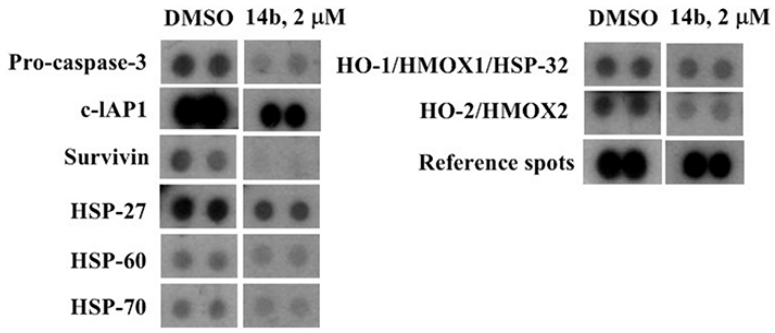

Scheme 1

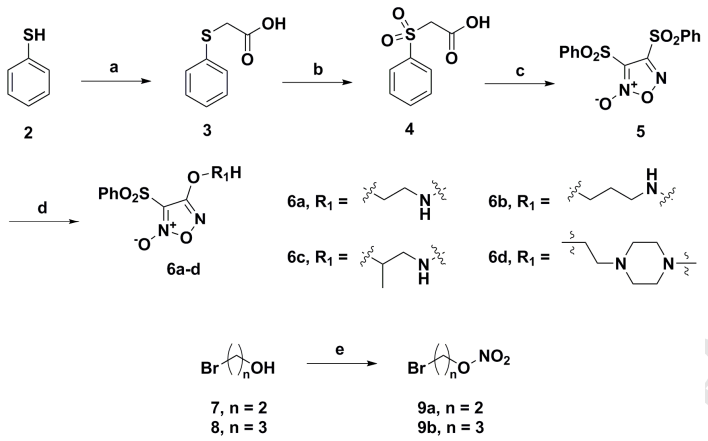

Scheme 2

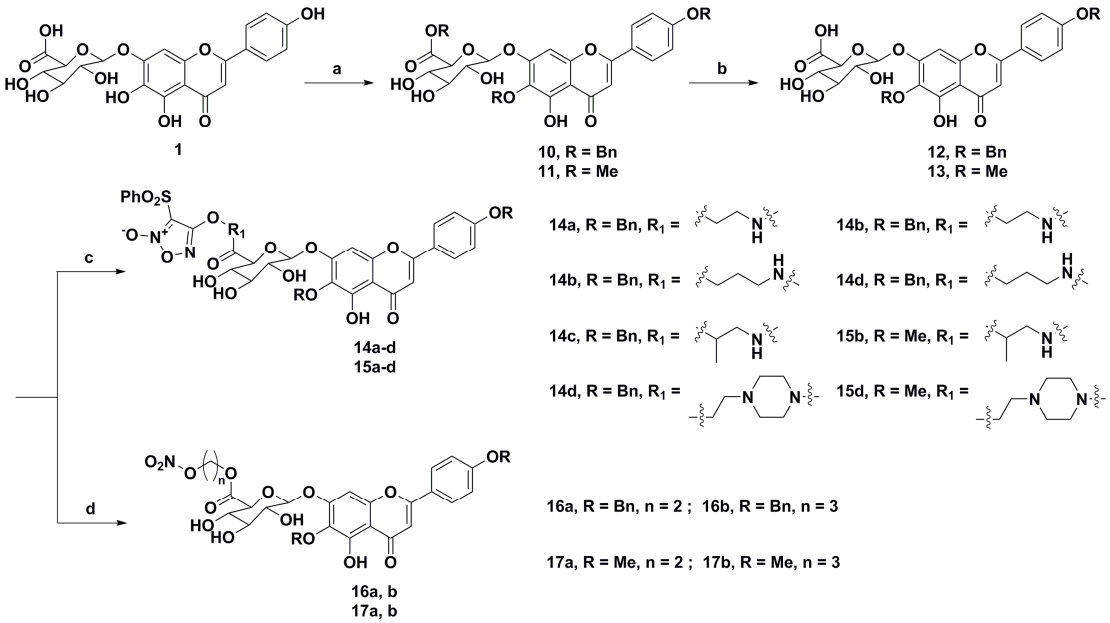

Highlights

- NO-releasing scutellarin derivatives were synthesized and biological evaluated.
- The SARs were concluded and the ability of NO released was detected.
- Compounds **14b** exhibited remarkable cytotoxicity and good selectivity.
- Compound **14b** arrested HepG2 cells at the S phase and induced apoptosis.
- The effects of compound **14b** on apoptosis-related proteins were disclosed.